

## Far-infrared signature of animal tissues characterized by terahertz time-domain spectroscopy

Mingxia He <sup>a,b</sup>, Abul K. Azad <sup>a</sup>, Shenghua Ye <sup>b</sup>, Weili Zhang <sup>a,\*</sup>

<sup>a</sup> School of Electrical and Computer Engineering, Oklahoma State University, 202 Engineering South, Stillwater, OK 74078, USA

<sup>b</sup> College of Precision Instrument and Optoelectronics Engineering, Tianjin University, Tianjin 300072, PR China

Received 7 May 2005; received in revised form 12 August 2005; accepted 14 August 2005

### Abstract

We present terahertz time-domain spectroscopy characterization of various animal tissues obtained from pork and rats. As the sensitivity of terahertz radiation to polar molecules of water is very high, biological tissues with high level of hydration show strong absorption at terahertz frequencies. The experimental data indicate that skin, fat and lean pork tissues have different frequency-dependent response to terahertz radiation due to the variation in water content. The same type tissue from different animals, however, is observed to show very similar water absorption.

© 2005 Elsevier B.V. All rights reserved.

PACS: 42.65.Re; 87.80.–y

Keywords: Terahertz time-domain spectroscopy; Animal tissue; Water content; Absorption

Terahertz radiation, generally defined by the frequency range of 0.1–10.0 THz, is an intriguing electromagnetic wave. Owing to the non-ionizing, non-invasive, coherent quasi-optic, and phase-sensitive properties, terahertz radiation has wide range applications in spectroscopy, imaging, and sensing. There has been an increasing interest in using terahertz time-domain spectroscopy (THz-TDS) to study systems of biomedical significance, particularly in genetic analysis, and cancer diagnosis [1–7].

Since many protein and DNA molecules have distinct signatures in the terahertz spectral region, THz-TDS has been used to identify various types of DNA from low frequency vibrational modes toward label free genetic diagnosis. Recently, various terahertz imaging techniques have been developed and demonstrated in the diagnosis of human and animal tumors. Terahertz pulse imaging (TPI) has been applied to identify human skin cancer, basal cell carcinoma (BCC) both in vitro and in vivo [8,9]. By analyzing

the image data from both time-domain and frequency-domain, the border zone between normal and diseased tissue can be well determined by TPI. Terahertz dark-field imaging of canine cancerous tissue has been reported which also demonstrated the promising capability of terahertz imaging in tumor detection and diagnosis [3].

As well known that water shows strong absorption at terahertz frequencies ( $\alpha = 200 \text{ cm}^{-1}$  at 1.0 THz) [10,11]. Biomedical tissues with different water content have different response to terahertz radiation. The application of terahertz imaging in cancer diagnosis is based on the fact that THz-TDS is capable to differentiate between diseased and normal tissue owing to the variation in water content. Since cancerous tissue has higher hydration compared to healthy tissue, it shows increased absorption in the terahertz spectral region. This enables tumor diagnosis using terahertz imaging modality with reasonably high contrast.

Theoretical simulation has also confirmed that water plays a major role in distinction between diseased and normal tissue [10]. Different types of normal tissues, however, have different water content as well. By looking at

\* Corresponding author. Tel.: +1 405 744 7297; fax: +1 405 744 9198.  
E-mail address: [wzhang@okstate.edu](mailto:wzhang@okstate.edu) (W. Zhang).

the transmission properties, one can obtain the terahertz signatures of various biomedical tissues. In this paper, we present terahertz transmission characterization of animal tissues taken from pork and rats. The power absorption data derived from THz-TDS measurements reveal clear distinction between different types of tissues.

The THz-TDS experimental setup is illustrated in Fig. 1. The generation and detection of terahertz electromagnetic pulses employ photoconductive switching of transmitter and receiver. Femtosecond, 800-nm optical pulses generated from a self-mode-locked Ti:Sapphire laser are used to gate the photoconductive switches. The terahertz setup has four parabolic mirrors arranged in an 8-F confocal geometry [12]. The terahertz beam emitted from the GaAs transmitter is spatially gathered by a silicon lens and then collimated into a parallel beam by the parabolic mirror,  $M_1$ . In order to compress the terahertz beam to a diameter comparable to the size of small samples, an additional pair of  $f=50$  mm parabolic mirrors,  $M_2$  and  $M_3$  are placed midway between the two major parabolic mirrors,  $M_1$  and  $M_4$ . The beam is re-collimated after leaving  $M_3$  and focused into another silicon lens at the silicon-on-sapphire (SOS) receiver end by  $M_4$ . This 8-F confocal system not only ensures excellent beam coupling between the transmitter and receiver but also compresses the terahertz beam to a frequency independent diameter of 3.5 mm. The THz-TDS system has a useful bandwidth of 0.1–4.5 THz (3 mm–67  $\mu$ m) and a signal to noise ratio (S/N) of >10000:1.

Two groups of animal samples are characterized. Group I includes skin, fat and lean tissue of pork; group II includes skin and lean tissue of rats. Prior to the THz-TDS measurements, the tissues were sliced into thin and parallel slabs with area dimensions of 10 mm  $\times$  10 mm after being frozen for few hours. In order to accurately determine the sample thickness, as well as the power absorption coefficient, the thawed tissue was gently placed in between two 636- $\mu$ m thick high-quality silicon slabs with a p-type resistivity of 20  $\Omega$  cm. The tissue thickness was obtained by measuring the thickness of the silicon-tissue-silicon sandwich using a Mitutoyo table-top micrometer and each thickness data was an average of 10 measurements. In

the THz-TDS experiments, a silicon–air–silicon sandwich with identical thickness was used as a reference.

Fig. 2 shows the schematic diagram of the reference- and sample-silicon sandwiches.  $E_{ref}(\omega)$  and  $E_{tis}(\omega)$  represent the Fourier transformed spectra of the transmitted terahertz pulses from the reference and tissue sample, respectively. The transmitted time-domain terahertz pulses and the corresponding spectra of the reference and the pork tissues are shown in Fig. 3. The tissue samples characterized here include fat, skin and lean tissues of pork with thickness of 1.10, 1.14 and 1.09 mm, respectively. As the results of optical dispersion and the frequency-dependent absorption, the terahertz pulses shown in Fig. 3(a) have different level of broadening, phase shift and amplitude attenuation as propagated through the tissue samples. Due to high water content the skin and lean tissues show very weak terahertz signals that are multiplied by 700 to compare with the amplitude signal of reference. The fat tissue, however, owing to very low level of hydration, shows strong transmission signal which is more than two orders of magnitude higher than that from skin and lean tissues. On the other hand, we observe that the terahertz signal from skin tissue is obviously stronger compared to that from lean tissue, which is also resulted from the difference of water content. As water absorption increases with increasing terahertz frequency, the transmission spectra of skin and lean tissues

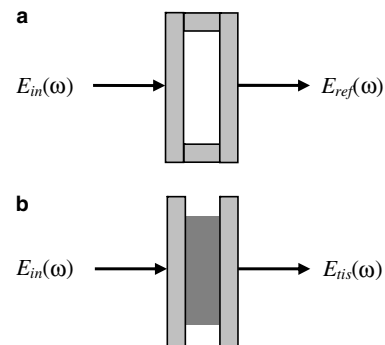


Fig. 2. (a) Reference silicon cell made of silicon–air–silicon sandwich; (b) identical silicon cell filled with animal tissue.

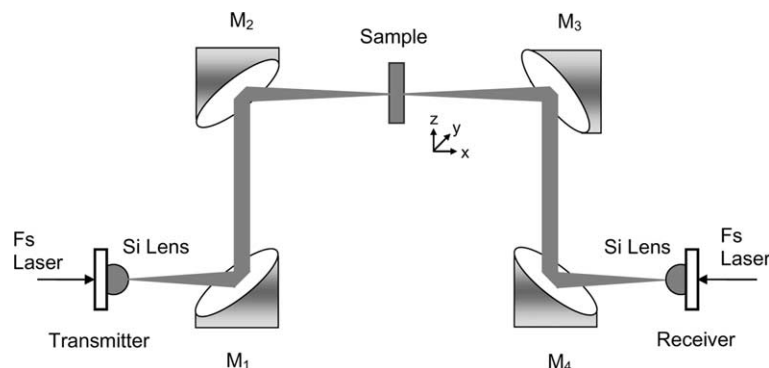


Fig. 1. Schematic diagram of the THz-TDS setup with 8-F confocal geometry. The tissue sample to be characterized is placed at the minimum waist position.

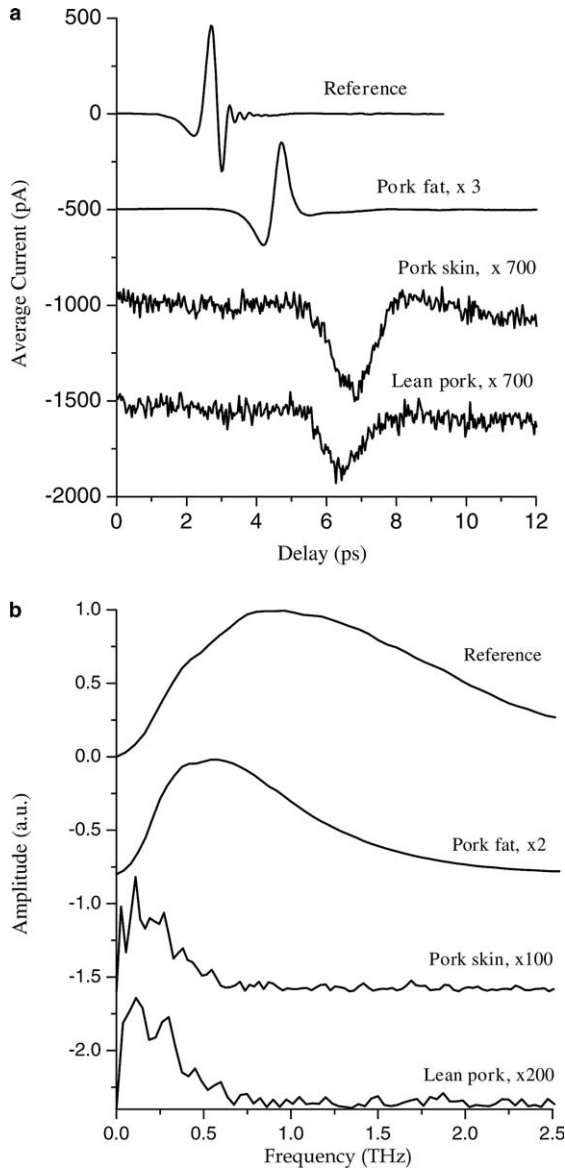


Fig. 3. THz-TDS curves of pork tissues. (a) Transmitted terahertz pulses of reference, fat, skin and lean tissues of pork; (b) the corresponding Fourier-transformed spectra. The thickness of the measured samples is 1.10 mm (fat), 1.14 mm (skin) and 1.09 mm (lean pork), respectively. The curves are vertically displaced for clarity.

plotted in Fig. 3(b) show very narrow bandwidth, indicating that such tissues with 1-mm thickness are nearly opaque to terahertz radiation at frequencies above 0.7 THz.

The power absorption of the animal tissues is extracted based on the transmitted pulses. Because of the clear separation in time domain between the transmitted and the first reflected pulse, the multiple reflection effect of the sandwiches is ignored in the data analysis. The complex transmission spectra of the reference  $E_{ref}(\omega)$  and the tissue sample  $E_{tis}(\omega)$  are given by:

$$E_{ref}(\omega) = E_{in}(\omega)t_{sa}t_{as}(ik_0d), \tag{1}$$

$$E_{tis}(\omega) = E_{in}(\omega)t_{st}t_{ts}(ikd)(-\alpha d/2), \tag{2}$$

where  $E_{in}(\omega)$  is the incident pulse spectrum,  $k_0 = 2\pi/\lambda_0$  and  $k = 2\pi n_t/\lambda_0$  are the wave vectors for air and sample, respectively;  $n_t$  is the refractive index of the tissue sample,  $d$  is the sample thickness,  $\lambda_0$  is the free-space wavelength, and  $\alpha$  is the power absorption coefficient of the tissue;  $t_{sa}$ ,  $t_{as}$ ,  $t_{st}$ , and  $t_{ts}$  are the Fresnel transmission coefficients of the terahertz pulses propagating through silicon–air, air–silicon, silicon–tissue, and tissue–silicon interfaces, respectively, which are given by  $t_{sa} = 2n_s/(1 + n_s)$ ,  $t_{as} = 2/(1 + n_s)$ ,  $t_{st} = 2n_s/(n_s + n_t)$ , and  $t_{ts} = 2n_t/(n_s + n_t)$ . The  $t_{st}$  and  $t_{ts}$  are the complex, frequency-dependent coefficients related to the tissue samples.

Fig. 4 shows the power absorption coefficients of the pork samples. Among different types of the pork tissues, lean pork shows the highest absorption and the frequency-dependent value is comparable with the previous measurement of pork-muscle tissue [13]. As being consistent with the estimation from the time-domain transmitted pulse and the corresponding spectra, the absorption coefficient of skin tissue is obviously lower than that of lean pork by an average of 10%. Compared to skin and lean pork, the fat tissue shows extremely low absorption at terahertz frequencies due to very low water content. At 0.5 THz, the power absorption coefficients of skin and lean pork are all above  $100 \text{ cm}^{-1}$ , while it is only  $15 \text{ cm}^{-1}$  for pork fat. Clearly, the power absorption coefficient provides a quantitative response of the tissue samples to terahertz radiation, which enables the differentiation of various types of biological tissues using terahertz spectroscopy technique.

We have also carried out THz-TDS characterization of rat tissues. The experimental procedure was essentially the same as described above. The tissues were measured within 24 h of the euthanasia of the six-month-old rats. The skin and lean tissues with thickness of 0.53 and 0.96 mm, respectively, were characterized. As shown in Fig. 5, the power absorption coefficients of the rat tissues have very similar values compared to the results obtained in pork tissues.

In conclusion, the THz-TDS transmitted time-domain pulses, the Fourier transformed spectra, and the derived

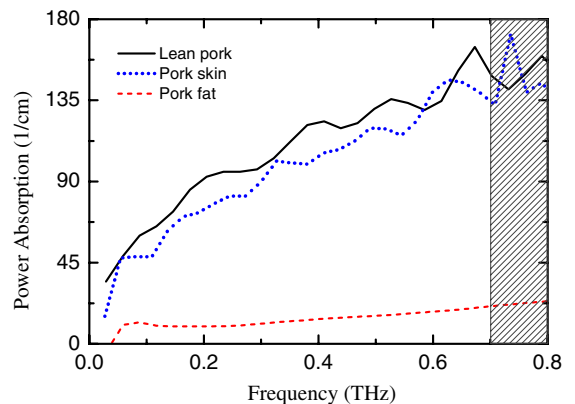


Fig. 4. Power absorption coefficients of pork tissues. Measurements are not considered accurate in the shaded area.

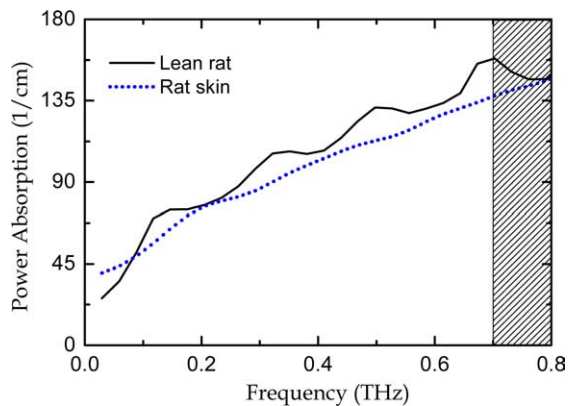


Fig. 5. Power absorption coefficients of rat tissues. The thickness of the skin and lean rat tissues is 0.65 and 0.96 mm, respectively.

power absorption coefficients enable the differentiation between different types of animal tissues. The same type tissue of different animals, however, shows similar terahertz response. The measured lean tissues of pork and rats have similar value of frequency-dependent power absorption which is also consistent with the previous data on pork-muscle. The obvious terahertz signatures observed for different type of animal tissues further demonstrate the feasibility of using terahertz technology in the biomedical applications.

We thank G.P. Chen for helpful discussions and J.L. Pope for providing the rat tissue samples. This work was partially supported by the Oklahoma EPSCoR for the National Science Foundation of US, and the China Scholarship Council.

## References

- [1] B. Ferguson, X.-C. Zhang, *Nature Mater.* 1 (2002) 26.
- [2] R.M. Woodward, B.E. Cole, V.P. Wallace, R.J. Pye, D.D. Arnone, E.H. Linfield, M. Pepper, *Phys. Med. Biol.* 47 (2002) 3853.
- [3] T. Löffler, T. Bauer, K.J. Siebert, H.G. Roskos, A. Fitzgerald, S. Czausch, *Opt. Express* 9 (2001) 616.
- [4] A.G. Markelz, A. Roitberg, E.J. Heilweil, *Chem. Phys. Lett.* 320 (2000) 42.
- [5] M. Walther, B. Fischer, M. Schall, H. Helm, P. Uhd Jepsen, *Chem. Phys. Lett.* 332 (2000) 389.
- [6] M. Brucherseifer, M. Nagel, P.H. Bolivar, H. Kurz, A. Bosserhoff, R. Büttner, *Appl. Phys. Lett.* 77 (2000) 4049.
- [7] J. Nishizawa, T. Sasaki, K. Suto, T. Yamada, T. Tanabe, T. Tanno, T. Sawai, Y. Miura, *Opt. Commun.* 244 (2005) 469.
- [8] R.M. Woodward, V.P. Wallace, R.J. Pye, B.E. Cole, D.D. Arnone, E.H. Linfield, M. Pepper, *J. Invest. Dermatol.* 120 (2003) 72.
- [9] B.E. Cole, R.M. Woodward, D. Crawley, *Proc. SPIE* 4276 (2001) 1.
- [10] E. Pickwell, B.E. Cole, A.J. Fitzgerald, V.P. Wallace, M. Pepper, *Appl. Phys. Lett.* 84 (2004) 2190.
- [11] J. Zhang, D. Grischkowsky, *Opt. Lett.* 29 (2004) 1617.
- [12] L. Thamizhmani, A.K. Azad, Jianming Dai, W. Zhang, *Appl. Phys. Lett.* 86 (2005) 131111.
- [13] P.Y. Han, G.C. Cho, X.-C. Zhang, *Opt. Lett.* 25 (2000) 242.